Inhomogeneous magnetic states in Fe and Cr substituted LaMnO$_3$

Inhomogeneous magnetic states in Fe and Cr substituted LaMnO$_3$

D V Karpinsky[1,3], I O Troyanchuk[1] and V V Sikolenko[2]

[1] Institute of Solid State and Semiconductor Physics, National Academy of Sciences, Brovki Street 19, Minsk 220072, Belarus
[2] Berlin Neutron Scattering Center, Hahn-Meitner-Institute, Glienicker Straße 100, D-14109 Berlin, Germany

E-mail: karpinsky@ifttp.bas-net.by

Abstract
Magnetization and neutron diffraction measurements have been performed on LaMn$_{0.5}$Fe$_{0.5}$O$_{3+d}$ and LaMn$_{0.5}$Cr$_{0.5}$O$_{3+d}$ perovskites. Neutron diffraction study revealed a G-type antiferromagnetic component as well as a ferromagnetic one for both stoichiometric compounds. Magnetic structure refinement for the LaMn$_{0.5}$Fe$_{0.5}$O$_3$ compound was performed on the basis of the three different models: noncollinear, multiphasic and ferrimagnetic. The reliability factors obtained for the Fe doped LaMnO$_3$ nearly coincide for the mentioned models and there are certain difficulties in preferring one of them. The magnetic moments calculated for these compounds have smaller values than the theoretically estimated ones, which can be explained by a magnetically frustrated phase within the samples. Magnetic properties can be well described using a superexchange mechanism. This model supposes Mn^{3+}–O–Mn^{3+} ferromagnetic interactions when static Jahn–Teller distortions are removed, whereas Cr^{3+}–O–Cr^{3+} and Fe^{3+}–O–Fe^{3+} interactions are strongly antiferromagnetic.

1. Introduction

LaMnO$_3$ is a perovskite-like A-type antiferromagnetic insulator with T_N about 140 K. Below T_N, spins of the Mn^{3+} ions are ordered ferromagnetically within the *ab*-plane but antiferromagnetically stacked along the *c*-axis. The ferromagnetism induced in this compound, either by oxygen nonstoichiometry [1, 2] or by divalent substitution of La ions [3–6], is traditionally explained in terms of a double exchange mechanism. This model considers the magnetic coupling between Mn^{3+} and Mn^{4+} ions as result of the motion of an e$_g$ electron between two partially filled d shells. However, ferromagnetism arises not only in the Mn^{4+}

---

[3] Author to whom any correspondence should be addressed.

doping case but also when Mn^{3+} ions are substituted by isovalent Ga^{3+}, Fe^{3+} or Cr^{3+} ions. Some authors [7, 8] have suggested that ferromagnetism observed in $LaMn_{1-x}M_xO_3$ systems (Cr^{3+}, Fe^{3+}) can be explained in terms of a superexchange model according to which removal of Jahn–Teller distortions leads to ferromagnetic interactions. The authors of [9–11] explained Mn^{3+}–Cr^{3+} and Mn^{3+}–Fe^{3+} interactions in $LaMn_{1-x}M_xO_3$ systems in terms of a double exchange model.

The magnetic properties for $LaMn_{1-x}M_xO_3$ systems (M = Cr^{3+}, Fe^{3+}) strongly depend on the preparation conditions, thus complicating an interpretation of their properties. It is possible that such an ambiguity can be explained in terms of cation ordering, which plays a crucial role in the magnetic and transport properties of the perovskite compounds. Dea *et al* [7] claimed an absence of any ordered structure in the compound $LaMn_{0.5}Fe_{0.5}O_3$ which exhibits a spin glass behaviour with an anomaly at 260 K. To the best of our knowledge the only ordered structure observed in these compounds is that in thin film $LaMn_{0.5}Fe_{0.5}O_3$ [12]. Ueda *et al* [12] declared an ordered state of B cations in the aforementioned compound with a rather high magnetic transition temperature (about 380 K) caused by Fe^{2+}–Mn^{4+} charge disproportion. The partly ordered structure of the $LaMn_{0.5}Cr_{0.5}O_3$ compound was noted by Bents [13], but recently this idea was discarded [8, 11].

One more aspect which has an influence on the magnetic and crystal structure of $LaMn_{1-x}Fe(Cr)_xO_3$ solid solutions is oxygen stoichiometry, e.g. a $LaMnO_3$ sample prepared in air has an oxygen content up to 3.11 [14] caused by the formation of cation vacancies. It is known that Fe ions usually have a 3+ high spin valence state in such compounds (this has been confirmed by Mossbauer measurements [7, 15]), whereas Mn ions can change their oxidation state to maintain electroneutrality of the compound. Thus Mn^{3+}–Mn^{4+} interactions can essentially modify the magnetic properties of the compound. In perovskite-like compounds the most probable valence state of the Cr ions is 3+. So one should bear in mind the possible deviations in the oxygen content to obtain the actual valence of the ions in $LaMn_{1-x}Fe(Cr)_xO_3$ systems.

In the present work an attempt was made to clarify the magnetic and crystal structures of $LaMn_{0.5}Fe_{0.5}O_{3+d}$ and $LaMn_{0.5}Cr_{0.5}O_{3+d}$ compounds as well as to analyse the origin of ferromagnetic interactions by means of neutron diffraction.

2. Experimental section

Polycrystalline samples of $LaMn_{0.5}Fe(Cr)_{0.5}O_{3+d}$ were prepared by a conventional solid state reaction method. The appropriate amounts of La_2O_3, Mn_2O_3, Cr_2O_3 and Fe_2O_3 were ground and calcined at 1420 K for 6 h. The calcined samples were then ground again, sintered at 1790 K for 2 h and cooled down to room temperature at a slow rate. Some of the samples were reduced in evacuated quartz ampoules at 1170 K for 24 h. Metallic tantalum was used as an oxygen getter. The neutron diffraction study was carried out using the FIREPOD diffractometer ($\lambda = 1.7971$ Å) at the Hahn-Meitner Institute (BENSC, Berlin). The phase purity of the samples was analysed using the DRON-3M x-ray diffractometer with Cu Kα irradiation. The structures were refined by the full-pattern Rietveld method using the program 'FullProf' [16]. Magnetic measurements were performed using a MPMS SQUID magnetometer (Quantum Design).

3. Results

The x-ray patterns indicate that all the samples of both series are single phase and have an orthorhombically distorted perovskite structure. The oxygen loss led to a certain increase
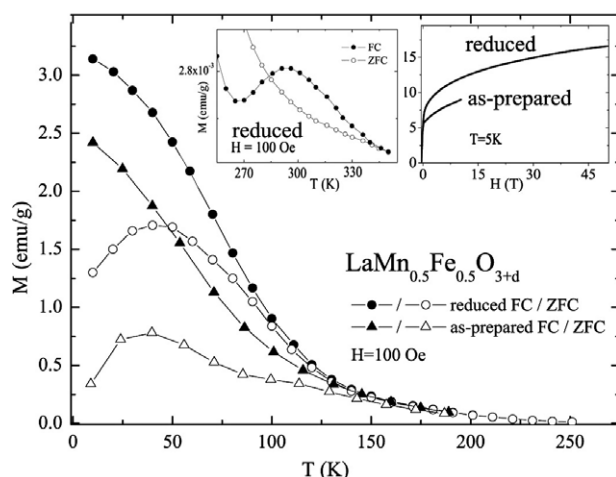
Figure 1. Temperature dependences of the magnetization for the LaMn$_{0.5}$Fe$_{0.5}$O$_{3+d}$ samples measured at $H = 100$ Oe. Filled and opened circles correspond to the reduced sample measured in FC and ZFC modes, respectively; the triangle symbols mean the same procedures for the as-prepared sample. The insets show the $M(H)$ dependence for both the samples (the as-prepared sample has been measured up to 15 kOe only) and anomalous behaviour of ZFC curve for the reduced sample.

in unit cell volume, confirmed by computer fitting of the neutron powder diffraction (NPD) patterns. The estimated mass loss of the samples after treatment in a vacuum corresponds to a decrease in oxygen content of 2% for both samples; it is worth noting that the increase in the unit cell volume is more pronounced for the LaMn$_{0.5}$Cr$_{0.5}$O$_{3+d}$ sample (about 1% for the Cr-doped compound, whereas for the Fe-doped one an increase in unit cell volume of about 0.2% has been estimated). Based on the oxygen content of the extreme members of LaMn$_{1-x}$Fe$_x$O$_3$ and LaMn$_{1-x}$Cr$_x$O$_3$ systems we have estimated this value for those compounds with an intermediate concentration prepared in air. The computer refinement of the NPD data confirmed a nearly stoichiometric composition of the reduced samples.

The magnetic measurements have been performed using both field cooled (FC) and zero-field cooled) ZFC procedures and the results are shown in figures 1 and 2. The oxygen reduction led to certain changes in the magnetic properties of the samples. Addressing the magnetization curves for the LaMn$_{0.5}$Fe$_{0.5}$O$_{3+d}$ compound we should notice that they resemble those observed in [17] where spin glass behaviour of the sample was declared. Both the reduced and the as-prepared samples have a smeared magnetic transition and branching point near the same temperature ($\sim$180 K) but the reduced one has a less pronounced divergence between the FC and ZFC curves, possibly testifying to a smaller inhomogeneous magnetic component in comparison with the as-prepared sample.

In spite of similar trends of the magnetization curves the reduced sample apparently possesses a stronger ferromagnetic component, as is confirmed by the $M(H)$ curve and by the shift of the ZFC maximum towards higher temperatures. The anomalous increase of the ZFC curve near 300 K is shown in the inset of figure 1, which assumes a certain magnetic phase segregation in the sample.

The coercive fields observed for these compounds are moderate (1 kOe for the as-prepared sample, 0.5 kOe for the reduced one), which is in accordance with the proposed magnetically inhomogeneous phase. The essential role of inhomogeneous phases is supported by field magnetization measurements, as even at relatively high magnetic fields (up to 5 T for the
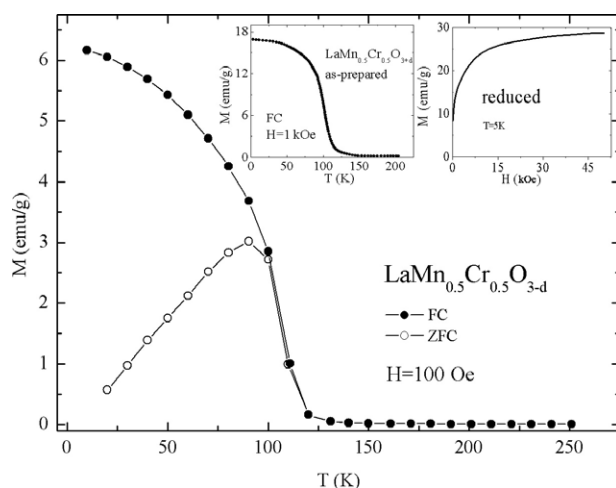
Figure 2. Temperature dependences of the magnetization for the LaMn$_{0.5}$Cr$_{0.5}$O$_3$ sample measured at H = 100 Oe. Filled and opened circles correspond to the FC and ZFC procedures. The right inset shows the $M(H)$ dependence. The left one demonstrates the $M(T)$ dependence for as-prepared LaMn$_{0.5}$Cr$_{0.5}$O$_{3+d}$ (data taken from [8]).

reduced sample) no saturation was observed. The spontaneous magnetization estimated from the field magnetization curves testifies to an increased magnetic moment (more than 0.6 μ_B) for the reduced sample. Nearly the same ferromagnetic moment has been calculated using the neutron data.

The magnetization curves for the reduced LaMn$_{0.5}$Cr$_{0.5}$O$_3$ compound closely resemble those mentioned for the as-prepared one in [8], indicating almost no changes after the sample treatment in a vacuum. According to magnetization data one can suggest certain ferromagnetic phases in the reduced sample with a magnetic transition temperature of about 120 K. The LaMn$_{0.5}$Cr$_{0.5}$O$_3$ compound has a narrowed magnetic transition in comparison with the LaMn$_{0.5}$Fe$_{0.5}$O$_3$ one. The coercive field observed for LaMn$_{0.5}$Cr$_{0.5}$O$_3$ is about 0.25 kOe, which is typical for a magnetically soft material. The field magnetization dependence shows near saturation at 5 T and the estimated magnetic moment of about 1.2 μ_B is close to that calculated from NPD data.

Rietveld analysis of NPD patterns for the LaMn$_{0.5}$Fe$_{0.5}$O$_{3+d}$ samples at 300 and 4.2 K has been performed assuming orthorhombic space groups as declared in [17], we managed to reach rather good reliability factors using this symmetry (space group *Pbnm* (no. 62)), so there is no evidence of B-ion ordering (some crystallographic parameters are shown in table 1). The maximum difference in M–O distances does not exceed 4%. The difference in the M–O distances becomes weakly pronounced at high temperature, indicating removal of the distortions of the oxygen octahedron. The unit cell parameters calculated are close to those obtained in [17].

The oxygen loss for the LaMn$_{0.5}$Cr$_{0.5}$O$_{3+d}$ sample does not lead to significant changes in crystal structure despite a certain increase in the unit cell volume. Both the reduced and the as-prepared samples can be well fitted assuming the orthorhombic *Pbnm* space group. The calculated M–O distances do not show any prominent difference, either at low temperature or at 300 K. The obtained lattice parameters evidence O-type orthorhombic structure, confirming the removal of Jahn–Teller distortions.

We could not observe any crystal structure transition for either of the reduced samples as temperature decreased. The only changes in diffraction patterns are connected with the

Table 1. The results of NPD refinements for the reduced $LaMn_{0.5}Cr_{0.5}O_3$ and $LaMn_{0.5}Fe_{0.5}O_3$ samples.

	$LaMn_{0.5}Cr_{0.5}O_3$		$LaMn_{0.5}Fe_{0.5}O_3$	
Temperature	4.2 K	300 K	4.2 K	300 K
Space group	*Pbnm*	*Pbnm*	*Pbnm*	*Pbnm*
a	5.5203(8)	5.5286(1)	5.5322(5)	5.5415(4)
b	5.5093(4)	5.5112(3)	5.5634(4)	5.5618(1)
c	7.7918(1)	7.8016 (1)	7.8177(5)	7.8328(6)
β (deg)	236.97(7)	237.71(3)	240.61(8)	241.41(5)
La:	4c	4c	4c	4c
x	−0.0057(3)	−0.0042(4)	−0.0041(9)	−0.0045(8)
y	0.0275(2)	0.0237(5)	0.0321(7)	0.0294(4)
M:	4b	4b	4b	4b
O(1):	4c	4c	4c	4c
x	0.0699(4)	0.0693(6)	0.0708(2)	0.071 72
y	0.4931(5)	0.4916(6)	0.4890(9)	0.490 04
O(2):	8d	8d	8d	8d
x	0.7212(3)	0.7232(5)	0.2210(3)	0.2216(3)
y	0.2786(3)	0.2790(2)	0.2121(5)	0.2138(3)
z	0.0363(2)	0.0363(7)	−0.03911	−0.0376(7)
M(1)–O(1)	1.986	1.988	1.994	1.998
M(1)–O(2)	1.982	1.992	1.967	1.970
M(1)–O(2)	1.984	1.976	2.038	2.032
M(1)–O(1)–M(2)	157.46(3)	157.59(7)	157.07(3)	156.84(3)
M(1)–O(2)–M(2)	159.04(5)	159.23(5)	156.79(9)	157.56(10)
R_p (%)	5.68	5.77	4.82	4.47
R_{wp} (%)	7.41	7.62	6.26	5.62
R_{Bragg} (%)	4.86	7.55	5.89	5.70
Chi2	2.18	2.52	2.67	1.88
Magnetic moments models:				
'two-phase'	1st phase (25%)		1st phase (40%)	R_z: ±1.16(3) μ_B
	R_x: 2.26(8) μ_B;		R_x: 1.46(7) μ_B;	
	2nd phase (75%)		2nd phase (60%)	
	R_z: ±1.64(4) μ_B;		R_z: ±2.16(2) μ_B;	
'canting'			R_x: 0.68(5) μ_B;	
			R_z: ±1.74(2) μ_B;	
'ferrimagnetic'			R_z: −2.29(8) μ_B;	
			R_z: +1.33(8) μ_B;	

magnetic contribution. The low temperature patterns reveal certain magnetic components for both samples. The magnetic peaks start to increase at the low angles mostly and coincide with crystallographic ones, which is explained by a unit cell format.

The low temperature NPD patterns for the $LaMn_{0.5}Fe_{0.5}O_3$ and $LaMn_{0.5}Cr_{0.5}O_3$ reduced samples demonstrate a certain magnetic contribution which can be separated into ferromagnetic and antiferromagnetic parts. The antiferromagnetic peaks are noticeably observed from (101), (011), (013) and (121) Bragg positions (figure 3). Because of close allocation of the (101), (011) peaks and the not very high resolution of the diffraction instrument it is rather difficult to distinguish their intensity ratio, and thus we failed to determine the direction of the antiferromagnetic moment. But the variant of the magnetic structure which assumes the
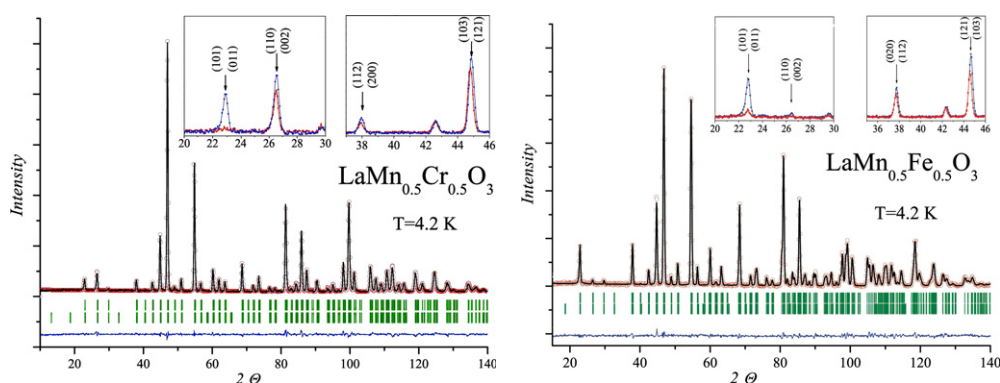
Figure 3. NPD refined patterns for the $LaMn_{0.5}Cr_{0.5}O_3$ (left) and $LaMn_{0.5}Fe_{0.5}O_3$ (right) samples recorded at 4.2 K. The observed intensities are shown by circles and the calculated ones by a solid line. The positions of the Bragg reflections are shown by the small vertical lines below the patterns (the upper lines denote crystal structure and the lower ones magnetic). The line at the bottom indicates the intensity difference between the experimental and the refined patterns. The comparison for the most informative peaks recorded at 300 and 4.2 K is shown on the inset.

(This figure is in colour only in the electronic version)

direction of the magnetic moment along the z axis gave slightly better reliability factors. The magnetic contribution contained in the mentioned reflections can be attributed to a G-type antiferromagnetic lattice like that declared in [18, 19]. The ferromagnetic component is mainly extracted from the (110), (200) reflections but because of the relatively small contribution its influence on the reliability factors is less pronounced.

In connection with complex properties of both $LaMn_{0.5}Fe_{0.5}O_3$ and $LaMn_{0.5}Cr_{0.5}O_3$ samples their magnetic structures have been examined in different models considered in the discussion section.

4. Discussion

Treatment of the samples in a vacuum allowed us to get nearly stoichiometric compounds as confirmed by computer refinement of the NPD data and thus to exclude any extra interatomic interactions with Mn^{4+} ions. Having stoichiometric compounds one can estimate intrinsic properties of the mentioned compounds whereas some authors [17] do not give much attention to this point. In the case of doping with Cr and Fe ions we deal only with interactions between mentioned transition metal ions in the 3+ valence state. Rather small (5–10%) substitution of Mn ions by Cr or Fe ones causes a suppression of the Jahn–Teller distortions and the degeneracy of the Mn^{3+} 3d energy levels is almost restored. But to drive such effects the admixture should be distributed homogeneously within the samples. The opposite situation is observed in [17] where doping of Fe ions by as much as 15% did not lead to any changes of the magnetic transition temperature. In the case of removed Jahn–Teller distortions dynamic ferromagnetic superexchange interactions Mn^{3+}–O–Mn^{3+} become valid and cause ferromagnetism. Further doping led to formation of strongly antiferromagnetic Cr^{3+}–O–Cr^{3+} and Fe^{3+}–O–Fe^{3+} interactions. So, the compounds with an intermediate doping level like $LaMn_{0.5}Fe_{0.5}O_3$ and $LaMn_{0.5}Cr_{0.5}O_3$ should demonstrate competition between ferromagnetic and antiferromagnetic interatomic interactions.

The complex magnetic behaviour of these solid solutions is seen from the magnetization curves. The $LaMn_{0.5}Fe_{0.5}O_3$ compound has a rather smeared magnetic transition to the

paramagnetic state. Such a gradual transition is evidence of a certain magnetic inhomogeneous phase like that observed in [7]. The thermomagnetic irreversibility and unsaturated behaviour of $M(H)$ at high magnetic fields (up to 5 T) also confirm the magnetically non-ordered component in the reduced sample. The moderate coercive field does not evidence any strong magnetic anisotropy. So the decreased value of the coercive field for the reduced sample can be explained by the smaller amount of the magnetically non-ordered phase in the latter compound. As the reduced compound almost has oxygen stoichiometry the positive superexchange interactions Mn^{3+}–O–Mn^{3+} become more pronounced, thus leading to an increase in magnetic moment.

Magnetization curves for the compound $LaMn_{0.5}Cr_{0.5}O_3$ demonstrate a coexistence of magnetically ordered and magnetically inhomogeneous phases. The spontaneous magnetization for this sample estimated from $M(H)$ is about 1.2 μ_B; this suggests a certain amount of a magnetically non-ordered phase in the sample. Assuming a ferrimagnetic order within the sample as claimed in [20] the theoretically estimated magnetic moment of this compound would be 1 μ_B (due to antiferromagnetic coupling between Mn^{3+} and Cr^{3+} ions with $3d^4$ and $3d^3$ electronic configurations, respectively) which is less than observed from $M(H)$ dependence, so a ferrimagnetic model would not be very useful for interpretation of the magnetic properties of this compound. Moreover, ferrimagnetism suggests an ordering in the B-cation positions, which in turn should affect the crystal structure of the compound, but there is no evidence of B-ion ordering observed on the NPD pattern. Because of the low magnetic anisotropy observed in the tested compound the next possible model—'canting'—has been also neglected as a non-collinear structure assumes rather strong material isotropy what is not observed for the mentioned compound.

One can obtain accurate data about the magnetic and crystal structure of the samples by using neutron diffraction. The crystal structure of the $LaMn_{0.5}Cr_{0.5}O_3$ compound at 300 K and 4.2 K has been calculated using the orthorhombic *Pbnm* space group. The magnetic structure of this compound has been estimated assuming the coexistence of ferromagnetic and antiferromagnetic components.

Reasonable reliability factors have been obtained in the so-called 'two-phase' model (see table 1). This model suggests a certain distinction between the phases, one of which is enriched with Cr ions and similar to an extreme member—$LaCrO_3$—whereas the other resembles non-stoichiometric $LaMnO_{3+d}$. The magnetic moments estimated from NPD data in the frames of this model are well correlate with the magnetization data and are listed in table 1 together with the estimated phase ratios. Competition between the mentioned magnetic phases possibly drives the magnetically frustrated phase but it does not play a key role in the magnetic properties of the compound.

The more contradictory situation is for the magnetic structure of the $LaMn_{0.5}Fe_{0.5}O_3$ solid solution. Magnetic structure fitting has been performed assuming three different models—noncollinear, multiphasic and ferrimagnetic. The estimated reliability factors are rather close between them but we can prefer one of them on the basis a set of characteristics assuming different physical backgrounds and thus causing different physical properties of the compound. According to the Kanamori–Goodenough rules, SE interactions Mn^{3+}–O–Fe^{3+} can be negative, and thus, in case of cation order, favour the formation of ferrimagnetic structure with an uncompensated magnetic moment of 1 μ_B. Magnetic moments obtained in the appropriate mathematical model can hardly be ascribed to Mn and Fe ions in a high spin valence state (see table 1). Moreover, the ferrimagnetic scenario suggests full ordering of the Mn and Fe ions, but in this case the cation order should affect the crystal structure, resulting in the appearance of a superstructure. Fitting of the NPD pattern does not suppose any cation ordering in the B-position of the perovskite structure. On the basis of the calculated NPD data we cannot draw a conclusion about the ordering of B-cations within the compound. So, assuming the coexistence

of ferrimagnetic and magnetically non-ordered phases one can roughly explain the parameters estimated from the magnetization measurements.

The next probable model describing the magnetic structure of the compound is a 'canting' one. The physical background of this model suggests essential magnetic anisotropy of the compound. But we did not observe strong magnetic anisotropy for this compound, which means that this model is uncertain. The computer variables used in this model (see table 1) determine the ferromagnetic moment along the x axis and the antiferromagnetic one is described by G-type structure along the z axis. It is actually difficult to appreciate the exact spatial orientation of the magnetic moments in the case of bulk materials, but the best reliability factors have been obtained by assuming the mentioned configuration.

The following model proposed to explain the magnetic properties is a 'two-phase' one, which suggests a certain distinction of the regions enriched in either Mn or Fe ions. These formations should exhibit properties resembling those of extreme members of the $LaMn_{1-x}Fe_xO_3$ system. In such a case we should observe some anomaly in the temperature dependence of magnetization due to competition between these phases. Such a prominent feature in the form of a small increase in the ZFC curve is really observed in the temperature range 280–300 K (figure 1); moreover, an antiferromagnetic moment of 1.2 μ_B has been estimated from the 300 K NPD pattern. The mentioned peculiarities can be driven by relaxation of the antiferromagnetic component. These anomalies resemble those for the extreme $LaFeO_3$ compound ($T_N = 750$ K) assuming a strength of G-type antiferromagnetic interactions that is two times lower. Low temperature calculations of the magnetic moments for both magnetic phases testify to the coexistence of Mn- and Fe-rich clusters close to extreme members of the $LaMn_{1-x}Fe_xO_3$ system. The calculated magnetic moments, as well as some unit cell parameters, are shown in table 1. Assuming 40% of the ferromagnetic phase the magnetic moment (1.5 μ_B) calculated for the 4.2 K NPD pattern is in good agreement with that obtained from magnetization data. The antiferromagnetic phase has a more relative part and persists above room temperature. Most probably its behaviour is governed by strong negative Fe^{3+}–O–Fe^{3+} interactions.

Dea *et al* [7] claimed a cluster glass-like behaviour of the $LaMn_{1-x}Fe_xO_3$ system, suggesting competition between distinct ferromagnetic and antiferromagnetic regions. Another confirmation of the phase separation model is the magnetic properties of the $LaMn_{1-x}Ga_xO_3$ system [21]. In [21] Blasco *et al* declare that diamagnetic dilution of Mn^{3+} ions by Ga^{3+} ions leads to evolution from canting antiferromagnetism to collinear ferromagnetism in the case of the $LaMn_{0.5}Ga_{0.5}O_3$ compound. The magnetic moment and characteristic magnetic transition temperature observed in [21] are close to those for $LaMn_{0.5}Fe_{0.5}O_3$, suggesting that the ferromagnetic component is of the same nature. Moreover the magnetic properties of $LaCo_{1-x}Fe_xO_3$ solid solutions [18] point to separation into magnetically active regions enriched with Fe^{3+} ions and those containing Co^{3+} which hardly show any active participation in the magnetic interactions. Phase segregation is probably a common feature of the mentioned compounds. The above-mentioned facts strongly incline us to favour the phase separation scenario for the $LaMn_{0.5}Fe_{0.5}O_3$ compound.

5. Conclusion

The magnetic properties of the $LaMn_{0.5}Fe_{0.5}O_3$ and $LaMn_{0.5}Cr_{0.5}O_3$ compounds have been analysed in terms of models assuming an inhomogeneous magnetic structure of these solid solutions. The magnetic properties of both compounds have been interpreted in terms of the 'two-phase' model supposing a certain segregation into ferromagnetic and antiferromagnetic regions. Some arguments in favour of the phase separation scenario have been proposed.

One can unambiguously determine the presence of ferromagnetic and antiferromagnetic components, but the nature of the magnetically non-ordered phase is still a matter of study. The observed interatomic interactions for both samples can be well explained in terms of the superexchange model assuming positive Mn^{3+}–O–Mn^{3+} interactions as well as negative Cr^{3+}–O–Cr^{3+} and Fe^{3+}–O–Fe^{3+} ones.

Acknowledgments

References

[1] Joy P A, Sankar C R and Date S K 2002 *J. Phys.: Condens. Matter* **14** 4985
[2] Ritter C, Ibarra M R, De Teresa J M, Algarabel P A, Marquina C, Blasco J, García J and Oseroff S 1997 *Phys. Rev.* B **56** 8902
[3] Malavasi L, Ritter C, Cristina M, Tealdi M C, Islam M S, Azzoni C B and Flor G 2005 *J. Solid State Chem.* **178** 2042
[4] Troyanchuk I O, Khalyavin D D, Solovykh T K, Szymczak H, Huang Q and Lynn J W 2000 *J. Phys.: Condens. Matter* **12** 2485
[5] Hibble S J, Cooper S P, Hannon A C, Fawcett I D and Greenblatt M 1999 *J. Phys.: Condens. Matter* **11** 9221
[6] Liu G D, Che G C, Zhao Z X, Jia S L, Guo S Q, Zhang Y Z, Chen H, Wu F and Dong C 1998 *J. Phys.: Condens. Matter* **10** 8477
[7] Dea K, Rayb R, Pandac R N, Giria S, Nakamurad H and Kohara T 2005 *J. Magn. Magn. Mater.* **288** 339
[8] Sun Y, Tong W, Xu X and Zhang Y 2001 *Phys. Rev.* B **63** 174438
[9] Tong W, Zhang B, Tan S and Zhang Y 2004 *Phys. Rev.* B **70** 014422
[10] Zhang L W, Feng G, Liang H, Cao B S, Meihong Z and Zhao Y G 2000 *J. Magn. Magn. Mater.* **219** 240
[11] Sun Y, Tong W, Xu X and Zhang Y 2001 *Phys. Rev.* B **63** 174438
[12] Ueda K, Muraoka Y, Tabata H and Kawai T 2001 *Appl. Phys. Lett.* **78** 512
[13] Bents U H 1957 *Phys. Rev.* **106** 225
[14] Topfer J and Goodenough J B 1997 *J. Solid State Chem.* **130** 117
[15] Jia Y Q, Liu S T, Wu Y, Jin M Z, Liu X W and Liu M L 1994 *Phys. Status Solidi* a **143** 15
[16] Rodríguez-Carvajal J 1993 *Physica* B **192** 55
[17] Joseph Joly V L, Bhame S D, Joy P A and Date S K 2003 *J. Magn. Magn. Mater.* **261** 433
[18] Karpinsky D V, Troyanchuk I O, Barner K, Szymczak H and Tovar M 2005 *J. Phys.: Condens. Matter* **17** 7219
[19] Peterlin-Neumaier T and Steichele E 1986 *J. Magn. Magn. Mater.* **59** 351
[20] Yang Z, Ye L and Xie X 2000 *J. Phys.: Condens. Matter* **12** 2737
[21] Blasco J, García J, Campo J, Sanchez M C and Subıas G 2002 *Phys. Rev.* B **66** 174431